The deubiquitinating enzyme Otu1 releases substrates from the conserved initiation complex of the Cdc48/p97 ATPase for proteasomal degradation

Hao Li[1]*, Haipeng Guan[1,2], and Tom A. Rapoport[1]*

[1] Department of Cell Biology, Harvard Medical School, and Howard Hughes Medical Institute; 240 Longwood Avenue, Boston, MA 02115, USA.

[2] Current address: Department of Biochemistry and Molecular Biophysics, Washington University in St. Louis, School of Medicine

*Corresponding authors: Hao_Li@hms.harvard.edu; Tom_Rapoport@hms.harvard.edu

Abstract

Many eukaryotic proteins are modified with a polyubiquitin chain and then recruited to either the Cdc48 ATPase (p97 or VCP in mammals) or the 26S proteasome by conserved cofactors. They can then shuttle between the Cdc48 ATPase and the 26S proteasome before being degraded. How substrates avoid being trapped on the Cdc48 ATPase complex is incompletely understood, as they can undergo repeated cycles of translocation through the ATPase pore. Here, we show that the deubiquitinating enzyme (DUB) Otu1 (Yod1 in mammals) can break this futile cycle. Otu1 trims the ubiquitin chain of the substrate before its translocation through the Cdc48 pore is initiated, allowing transfer to the proteasome and subsequent degradation. A cryo-EM structure shows that the mammalian homolog Yod1 binds to p97 simultaneously with other Cdc48 cofactors. As in the yeast system, polypeptide translocation through the ATPase pore is initiated by the unfolding of a ubiquitin molecule, suggesting that the mechanism of substrate processing is conserved in all eukaryotes.

Key words: AAA ATPase, p97/VCP, ubiquitin, deubiquitination, protein degradation

Introduction

Regulated protein degradation in eukaryotes generally begins with the attachment of a polyubiquitin chain[1]. If the target protein contains a flexible segment, it can directly be degraded by the 26S proteasome; the segment inserts into the pore of the 19S regulatory particle and initiates substrate transfer into the proteolytic chamber of the 20S core particle[2]. In contrast, well-folded proteins require initial unfolding, a step mediated by the ATPase Cdc48 in yeast and its homolog p97 in mammals (also called VCP)[3]. Cdc48/p97 consists of an N-terminal (N) domain and two ATPase domains, D1 and D2. Six Cdc48/p97 molecules assemble into a double-ring hexameric structure with a central pore. Substrate is recruited to one side of the Cdc48/p97 double-ring (the cis side) through binding of the attached ubiquitin chain to a cofactor, the heterodimeric Ufd1-Npl4 (UN) complex. A cryogenic electron microscopy (cryo-EM) structure of the yeast Cdc48-UN complex with polyubiquitinated substrate showed that one of the ubiquitin molecules in the chain (the initiator ubiquitin) is unfolded by binding to a groove in Npl4 and insertion of an N-terminal segment into the central pore of the ATPase[4]. Biochemical experiments indicated that no ATP-binding or -hydrolysis is required for the unfolding of the initiator ubiquitin[5]. In the next step, the D2 ring uses the energy of ATP hydrolysis to sequentially move the initiator ubiquitin, all ubiquitin molecules positioned between the initiator and the substrate, and finally the substrate itself through the pore, causing their unfolding. The ubiquitin molecules refold on the trans side, allowing a substrate to rebind to the Cdc48-UN complex, so that the ATPase can act again on a substrate that has already been translocated. How this futile cycle would be disrupted is poorly understood. Furthermore, additional structures are required to confirm the proposed mechanism of substrate processing, particularly because no unfolded ubiquitin was seen in recent structures of the substrate-engaged human p97-UN complex[6,7].

We have recently shown that a polyubiquitinated substrate can shuttle between the Cdc48/p97 complex and the 26S proteasome before being degraded[8]. Shuttling is facilitated by the proteasome cofactor Rad23 and the Cdc48 cofactor Ubx5, which both reversibly bind folded and unfolded substrates through the substrate-attached ubiquitin chain. Whether other proteins also participate in substrate shuttling between the two molecular machines is unknown, but a possible factor is the deubiquitinating enzyme (DUB) Otu1 (Yod1 in mammals), which binds through its UBX-like (UBXL) domain to Cdc48/p97. The function of Otu1/Yod1 has remained unclear. It was initially proposed that the deubiquitinating activity of Otu1 is required for polypeptide translocation through the central pore[9]. However, subsequent work demonstrated that the removal of the ubiquitin chain is not required[10]. An alternative model was therefore proposed, according to which Otu1 promotes substrate release from the Cdc48 ATPase, thereby

70 breaking the futile cycle of repeated substrate unfolding and facilitating the transfer to
71 the proteasome[10].

72 Here, we provide evidence for this model. Using a reconstituted degradation system
73 with purified proteins, we show that Otu1 releases polyubiquitinated substrates from the
74 Cdc48 ATPase by trimming the ubiquitin chain, allowing transfer to the 26S proteasome
75 and subsequent degradation. A cryo-EM structure of human homologs of the Cdc48
76 complex reveals that Yod1 stabilizes the p97-UN-substrate complex. As in the yeast
77 system, one of the ubiquitin molecules in the chain is unfolded. This initiator ubiquitin
78 molecule is bound to a groove in Npl4 and projects its N-terminus across both ATPase
79 rings, engaging the pore residues of the D2 ring. Thus, the initiation of substrate
80 translocation through the ATPase pore is evolutionarily conserved. Given that p97 is a
81 promising cancer drug target, the structure may also allow the development of specific
82 compounds that interfere with the formation of the ATPase complex.

83

84

85 **Results**

86 **Otu1 promotes substrate transfer from the Cdc48 complex to the 26S proteasome**

87 We first tested the effect of Otu1 on protein degradation using our previously developed
88 *in vitro* degradation assay that utilizes purified components[8]. We initially used as a
89 substrate Ub(n)-TAIL, a purified, polyubiquitinated protein that is labeled with a
90 fluorescent dye. It contains flexible N- and C- terminal segments that enable its direct
91 degradation by the 26S proteasome. When Ub(n)-TAIL was incubated with purified 26S
92 proteasomes, the substrate was degraded to low-molecular weight peptides (**Figure 1A**,
93 lane 2 versus 1). The addition of increasing concentrations of purified Otu1 led to
94 deubiquitination of Ub(n)-TAIL, as seen from the appearance of labeled bands of
95 increased mobility in SDS-PAGE (lanes 3-6). Interestingly, the efficiency of substrate
96 degradation was not affected (**Figure 1A**, lanes 3-6 versus 2), suggesting that Otu1
97 does not remove the entire ubiquitin chain. This conclusion is in agreement with
98 previous experiments showing that Otu1 releases substrate molecules with chains
99 containing up to ten ubiquitin molecules[9]. Our results show that the remaining ubiquitin
100 chain is sufficient for recognition by the proteasome**.**

101 The addition of the Cdc48-UN ATPase complex inhibited the degradation of Ub(n)-TAIL
102 (**Figure 1A**, lane 7 versus 2), consistent with Cdc48-UN competing with the 26S
103 proteasome for binding to polyubiquitinated proteins[8]. Importantly, Otu1 was able to
104 relieve this inhibition (**Figure 1A**, lanes 8-11 versus 7), suggesting that Otu1 can
105 release substrates that are trapped on the Cdc48-UN ATPase, thereby allowing their

106 degradation by the proteasome. Otu1 activity is stimulated by the Cdc48 complex,
107 consistent with previous results[9,11].

108 We next used as a substrate Ub(n)-FOLD, a polyubiquitinated protein lacking flexible
109 segments. This substrate requires Cdc48-dependent unfolding for proteasomal
110 degradation. When added together with the 26S proteasome and Cdc48-UN, Otu1
111 caused deubiquitination, but had only a minor effect on the degradation of Ub(n)-FOLD
112 (**Figure 1B**, lanes 3-4 versus 2). These results again suggest that Otu1 does not
113 remove the entire ubiquitin chain, allowing Cdc48-UN and the 26S proteasome to act on
114 the substrate. As expected, the addition of an enzymatically inactive Otu1 mutant (Otu1-
115 C120S) did not cause deubiquitination, but it also had no effect on substrate
116 degradation (lanes 5 and 6). Thus, regardless of whether Otu1 trims the ubiquitin chain,
117 the rebinding of substrate to Cdc48-UN does not effectively compete with substrate
118 transfer to the proteasome.

119 Next we added Ubx5, a Cdc48 cofactor that helps to recruit polyubiquitinated proteins to
120 Cdc48-UN and therefore counteracts the transfer of substrate to the proteasome[8]. Ubx5
121 inhibited the degradation of Ub(n)-FOLD (**Figure 1B**, lane 7 versus 2), consistent with
122 the sequestration of the substrate at the ATPase complex. The addition of Otu1
123 reversed this inhibition in a dose-dependent manner (**Figure 1B**, lane 8 and 9 versus 7),
124 whereas the enzymatically inactive Otu1-C120S mutant was without effect (lanes 10
125 and 11). Ubx5 also inhibited the degradation of Ub(n)-TAIL when Cdc48-UN was
126 present (**Figure 1C,** lane 3 versus 2), and again this inhibition was alleviated by Otu1
127 (lanes 4 and 5). These results suggest that trimming of the ubiquitin chain by Otu1
128 disfavors the rebinding of substrate to the Cdc48-UN-Ubx5 complex and therefore
129 stimulates substrate transfer to the proteasome.

130 Otu1 contains an UBXL domain that binds to the N domain of Cdc48. Deletion of this
131 domain (Otu1-ΔUBXL) reduced ubiquitin chain cleavage and rendered the protein
132 inactive in stimulating substrate degradation (**Figure 1D**, lane 6 versus 4). Thus,
133 substrate release from Cdc48-UN depends on both Otu1 binding to Cdc48 (**Figure 1D**)
134 and the deubiquitination activity of Otu1 (**Figure 1B**). These results are consistent with
135 previous ones showing that Otu1 has a significantly higher deubiquitination activity
136 when bound to Cdc48 (ref. [9]).

137 Next we tested whether Otu1 trims the polyubiquitin chain before substrate translocation
138 through the central pore of Cdc48. To this end, we used Cdc48 mutants defective in ATP
139 hydrolysis and translocation activity, a Walker A mutant in the D1 ring (K261A) and a
140 Walker B mutant in the D2 ring (E588Q)[9]. Wild-type (WT), K261A, and E588Q Cdc48
141 each inhibited the degradation of Ub(n)-TAIL, with K261A showing the strongest
142 inhibition (**Figure 1E**, lanes 4-6 versus 2). In all cases, Otu1 relieved the inhibition
143 caused by the Cdc48 variants (**Figure 1E**, lanes 7-9 versus 4-6). These results suggest

144 that ubiquitin chain trimming by Otu1 and substrate transfer from Cdc48 to the
145 proteasome can occur prior to initiation of substrate translocation through the ATPase
146 rings. Otu1 stimulates substrate dissociation from Cdc48, which otherwise is slow[8].

147 Pull-down experiments confirmed this conclusion. A complex of Cdc48-UN and
148 polyubiquitinated substrates was assembled on beads. After a washing step, the beads
149 were incubated with different combinations of 26S proteasomes, Rad23, and Otu1. 26S
150 proteasomes with or without Rad23 did not efficiently release ubiquitinated substrates
151 from Cdc48-UN, as shown by the large amount of substrate remaining on the beads
152 after the second incubation (**Figure 1G**, lanes 2-3 versus 1). However, the addition of
153 Otu1 caused much of the substrate to be released (**Figure 1G**, lanes 4-5 versus 1). The
154 additional presence of proteasomes had only a small effect (lane 5 versus 4). These
155 results indicate that Otu1-mediated deubiquitination directly leads to substrate release
156 from the Cdc48 ATPase.

157 **Cdc48 can simultaneously bind several cofactors**

158 Substrate release by Otu1 implies that it can bind to a Cdc48 complex that also contains
159 Ufd1, Npl4, and Ubx5. To investigate whether all four proteins can bind simultaneously,
160 we performed pull-down experiments with a FLAG-tagged version of a catalytically
161 inactive Otu1 mutant (Otu1-C120S-FLAG), which prevents cleavage of the
162 polyubiquitinated substrate. The experiments were performed in the presence of the
163 ATP-analog ATPγS to block Cdc48 function. The samples were subjected to
164 immunoprecipitation with anti-FLAG antibodies and analyzed by SDS-PAGE and
165 fluorescence scanning to detect substrate, and by Coomassie blue staining to identify
166 Cdc48 and the cofactors (**Figure 2A,** upper and lower panels, respectively). The results
167 show that Otu1 alone interacts only weakly with polyubiquitinated substrate (**Figure 2A**,
168 lane 1; upper panel). Substrate binding is drastically enhanced when Cdc48-UN is
169 added (lane 3 versus 1, upper panel). Coomassie-blue staining (lower panel) showed
170 that all components were bound. Importantly, Ubx5 did not bind to the Cdc48-UN-Otu1
171 complex unless polyubiquitinated substrate was added (lane 5 versus 4). These results
172 demonstrate that Cdc48, Ufd1, Npl4, Otu1, Ubx5, and a polyubiquitinated substrate can
173 assemble into a complex. The cofactors Npl4, Otu1, and Ubx5 all contain a UBX or
174 UBX-like domain that is essential for their interaction with Cdc48 ([8],[9],[12]; shown for Otu1
175 in **Figure 2B**). Each of these domains can interact with one of the six N domains of the
176 Cdc48 hexamer, explaining the simultaneous binding of these cofactors.

177 To test whether a similar supercomplex can form with the human components, we
178 purified p97, the homolog of Cdc48, human Ufd1 (hUfd1), human Npl4 (hNpl4), UBXN7,
179 the homolog of Ubx5, and Yod1, the homolog of Otu1 (**Figure 2C**; lanes 1-5). Pull-down
180 experiments were performed in the presence of ATPγS with an SBP-tagged version of
181 UBXN7, using again an enzymatically inactive mutant of the DUB (Yod1-C160S). After

182 incubation with streptavidin beads, the bound material was eluted with biotin and
183 analyzed by Coomassie blue staining (**Figure 2C**). As with the yeast components, a
184 complex containing all proteins was formed in the presence of polyubiquitinated
185 substrate (**Figure 2C**, lane 13).

186 **A cryo-EM structure of the substrate-engaged human p97 complex**

187 We used the human p97 complex to determine a cryo-EM structure, hoping that all
188 components would be visible. For structure determination we used a p97 mutant with a
189 Walker B mutation in D2 (E578Q) to slow substrate translocation and the catalytically
190 inactive Yod1-C160S mutant to prevent deubiquitination. Approximately 800,000
191 particles were subjected to heterogeneous refinement, 3D classification, and non-
192 uniform refinement, resulting in an overall density map of 2.97 Å resolution (**figure S1**).
193 The map was locally refined to 3.05 Å for the D1 ring and the tower formed by hNpl4.
194 Models were built for the ATPase subunits of the D1 and D2 rings and for the hNpl4
195 tower (**Figure 3A**).

196 hNpl4 is anchored to the D1 ATPase ring by its two Zn^{2+}-finger domains (ZF-1 and ZF-
197 2), a β-strand finger, and an N-terminal bundle (NTB) domain (**figure S2A**). These
198 interactions are similar to those of yeast Npl4 (ref.[4]), except that the NTB in mammals is
199 significantly shorter (**figure S2B**) and binds to D1 closer to the central pore (**figures**
200 **S2A** and **S2C**). In our structure the hNpl4 tower is fixed in a defined position and both
201 Zn^{2+}-fingers interact with D1, whereas other authors reported that the hNpl4 tower was
202 tilted to different degrees and ZF-2 was not always engaged[7]. The differences might be
203 due to the presence of an unfolded ubiquitin molecule and/or the additional presence of
204 Yod1 and UBXN7 in our structure.

205 Density for an unfolded ubiquitin molecule (unUb) was seen from the groove in Npl4 all
206 the way through both ATPase rings (**Figure 3A, 3B**). As in the yeast Cdc48 ATPase
207 complex[4], the Npl4 binding groove that has a prominent kink, dividing the groove into
208 upper and lower parts (**Figure 3B**). The upper part accommodates residues P38 to K48
209 of unUB in an unfolded conformation, whereas the lower part binds residues S19 to
210 P38, which includes the single helix of ubiquitin (residues I23 to Q31) that remains
211 folded (**Figure 3B**). Because the resolution of the mammalian complex is significantly
212 higher than that of the yeast complex (~3Å versus 4Å), many amino acid side chains
213 could be modeled. Most unUb-interacting residues in the hNpl4 groove are conserved,
214 as noticed before (ref). However, two differences to the yeast complex were observed
215 (**figure S2D**). First, F45 of unUb intercalates between F382 and H231, whereas this
216 residue does not contribute to the interaction in yeast Npl4. Second, K33 and R42 of
217 unUb bind to an acidic patch that includes E383 and D451, which is only present in the
218 groove of human Npl4. Binding to unUb also leads to a conformational change of the
219 Npl4 groove. In the isolated human UN complex, the lower groove of hNpl4 is

220 occluded[13]; in our active complex, two helices shift outwards, widening the groove so
221 that it can accommodate unUb (**figure S2E**).

222 The N-terminus of unUb extends through the central pore of p97 all the way to the D2
223 ring (**Figure 3B**). As in the yeast complex, the D1 ring pore loops adopt a planar
224 arrangement (**Figure 3C**), with the loops of subunits A, B, and C contacting the unfolded
225 ubiquitin chain (**Figure 3D; inset #1**). The D2 pore loops form a staircase, with subunit
226 A on top and subunit E on the bottom (**Figure 3D; inset #2**). Five of the loops contact
227 the polypeptide. This arrangement supports a model in which sequential ATP hydrolysis
228 by the D2 subunits allows the pore loops to function as a conveyer belt. In this model,
229 subunit A binds to the top of the polypeptide chain and the subunits then move
230 downwards, dragging the polypeptide chain with them. At the lowest position, subunit F
231 disengages from the substrate and becomes flexible (and invisible in our structures); it
232 can then move to the top position and start a new cycle.

233 Density for the N domains of p97 and for the UBXL domain of Npl4 was weak, but after
234 local classification and refinement, a particle class was obtained in which three N
235 domains were much more visible than the other three. The visible N domains are
236 associated with subunits A, C, and F of the hexameric ring (**Figure 4A**). This class also
237 displayed density for the Npl4 tower and for unUb in the central pore and it showed the
238 D2 ring in the staircase conformation characteristic of substrate engagement (**Figure**
239 **4A**). The three visible N domains are in the up-conformation that likely requires the
240 associated D1 subunits to be in the ATP-bound state[9]. Density associated with one of
241 the N domains (of subunit C) was visible, but did not allow an unambiguous assignment
242 to one of the three UBX-like domains (those of Npl4, Yod1, and UBXN7). However, the
243 density most likely belongs to UBXL domain of Npl4, because an AlphaFold[14]-model
244 docked into it places the C-terminus the domain only 20 amino acids from the Npl4
245 tower (**figure S3A**; **Figure 4A**). No density for the other two UBX or UBX-like domains
246 was visible, perhaps because the N domains are too flexible, but it is tempting to
247 speculate that they are bound to the visible N domains associated with subunits A and
248 F. Although UBX domains can bind to both the up- and down- conformations of N
249 domains[15,16], they might stabilize the up-conformation.

250 Density for two folded ubiquitin molecules (Ub1 and Ub2) was visible on the top of the
251 Npl4 tower (**Figure 4A;B**), as in previous structures obtained with polyubiquitinated
252 substrate[4]. These ubiquitin molecules follow unUb in the chain (distal ubiquitin
253 molecules). Interestingly, Ub2 was approximately at the same position as in the yeast
254 complex, but Ub1 was much closer to Ub2 (**Figure 4B**)[4]. In fact, in the yeast structure,
255 the two ubiquitin molecules are too far apart to be linked, suggesting that only Ub2 was
256 actually bound. In contrast, in the human complex K48 of Ub1 is close to the C-terminus
257 of Ub2 (**Figure 4C**), indicating that both Ub1 and Ub2 are bound to the top of the Npl4
258 tower.

259 As in the yeast complex[4,17], only a portion of Ufd1 is visible (the UT6 domain), whereas
260 the ubiquitin-binding UT3 domain is too flexible to visualize. The central part of the UT6
261 domain forms a loop that associates with Npl4 (**figure S3B**). The loop is slightly different
262 from that seen in the crystal structure of the UN complex in isolation (**figure S3B**)[13]. The
263 loop is preceeded by a SHP segment (SHP1) that likely binds to the N domain of
264 subunit A, as there is density for the linker region (**figure S3C**). The second SHP
265 segment (SHP2) is invisible, as in the yeast structure, but probably interacts with the N
266 domain of subunit F. The exact function of Ufd1 is still unclear, but it is required for
267 substrate translocation[10].

268

269 **Discussion**

270 Here we show that the deubiquitinating enzyme Otu1 trims the ubiquitin chain bound to
271 the Cdc48 ATPase complex, releasing substrates before they are translocated through
272 the central pore of the double-ring ATPase. The released substrate still carries sufficient
273 ubiquitin molecules for degradation by the 26S proteasome. Substrate dissociation from
274 Cdc48-UN and binding to the 26S proteasome are possible because the ATPase
275 complex requires slightly longer polyubiquitin chains than the proteasome (5 ubiquitin
276 molecules versus 3-4; the human p97 prefers even longer chains)[9,18]. The action of
277 Otu1 breaks the futile cycles of substrate translocation through the Cdc48 pore and
278 therefore facilitates substrate transfer from the ATPase to the proteasome. Otu1
279 belongs to a small group of DUBs that promotes, rather than counteracts, protein
280 degradation. This group includes Rsp11 that removes the ubiquitin chain from
281 substrates prior to their translocation into the proteolytic chamber of the proteasome[19,20].

282 Otu1 likely cooperates with Ubx5 and Rad23, the recruitment factors for Cdc48-UN and
283 the 26S proteasome, respectively. Polyubiquitinated substrate bound to the Cdc48-UN-
284 Ubx5 complex can spontaneously dissociate and then be recruited by the 26S
285 proteasome/Rad23 complex. However, when the ubiquitin chain is long, the rebinding of
286 substrate to the ATPase complex is favored, so that only a fraction of the substrate is
287 transferred to the proteasome for degradation. Otu1 reduces the efficiency of rebinding
288 to the ATPase complex and thus increases the efficiency of transfer and degradation.
289 Otu1 is not essential for the viability of *S. cerevisiae* cells[9,11], so it is either a facilitating
290 factor or only required under certain conditions. For example, Otu1 might reduce the
291 load of the Cdc48 ATPase complex when misfolded polyubiquitinated proteins
292 accumulate that bind to the ATPase but do not require unfolding.

293 Our model implies that Otu1 can bind to Cdc48 simultaneously with the cofactors Npl4,
294 Ufd1, and Ubx5, as well as polyubiquitinated substrate. This prediction is indeed
295 confirmed by pull-down experiments. Moreover, our experiments suggest that substrate
296 binding promotes the interaction of Cdc48 with the cofactors. This synergistic interaction

297 is also seen with the human proteins and is consistent with earlier results showing that
298 binding of the UN complex stimulates the binding of the human Ubx5 homolog[21].
299 However, it is likely that the cofactors are not always bound at the same time and could
300 associate with Cdc48/p97 in different combinations. How exactly substrate and the
301 cofactors cooperate requires a structure in which all components are visualized.

302 An important result of our study is the demonstration that the initiation of substrate
303 processing by the ATPase complex is evolutionary conserved. Our cryo-EM structure of
304 the human complex is quite similar to the one obtained with *S. cerevisiae* components.
305 As in yeast[4], one of the ubiquitin molecules in the chain (the initiator) is unfolded. This
306 ubiquitin molecule is bound to a groove in Npl4 and projects its N-terminal segment
307 across both ATPase rings. The interaction with the pore loops of the D2 ring indicates
308 that a conveyor belt mechanism is used to pull on the N-terminus of the initiator
309 ubiquitin. It remains unclear why recent cryo-EM structures of Cdc48-UN with SUMO–
310 polyubiquitin hybrid chains and of human p97-UN with polyubiquitinated substrate did
311 not show a ubiquitin segment in the central pore[22] or unfolded ubiquitin in Npl4 and the
312 pore[6,7].

313 Our structure supports a model in which the ATPase first moves the initiator ubiquitin
314 through the central pore, then all ubiquitin molecules positioned between the initiator
315 and the substrate (proximal ubiquitins), and finally the substrate itself. All polypeptides
316 moving through the central pore are unfolded, but the proximal ubiquitin molecules
317 refold when they emerge on the trans side of the double-ring ATPase. The distal
318 ubiquitin molecules are not translocated through the central pore and are therefore
319 never unfolded[5]. They likely move through lateral openings between two protomers of
320 the two ATPase rings.

321 p97 has long been considered a promising target of cancer drugs[23]. Inhibitors of p97
322 have entered clinical trials for solid tumors and myeloid leukemia, but toxicity remains
323 an issue[24]. Recent efforts have therefore focused on developing specific inhibitors that
324 disrupt the p97-UN complex. Thonzonium bromide has been shown to inhibit tumor
325 growth by binding to the interface between p97 and Npl4[25]. and peptide inhibitors
326 derived from Ufd1 compete with Npl4 for binding and inhibit the unfolding activity of the
327 p97-UN ATPase[26]. Our structure provides the basis for yet another approach in which
328 drugs would prevent the binding of unfolded ubiquitin to the Npl4 groove.

329

330

METHODS

RESOURCE AVAILABILITY

Lead Contact

Further information and requests for resources and reagents should be directed to and will be fulfilled by the Lead Contact, Tom Rapoport (tom_rapoport@hms.harvard.edu).

Materials Availability

All unique/stable reagents generated in this study are available from the Lead Contact with a completed Materials Transfer Agreement.

EXPERIMENTAL MODEL AND STUDY PARTICIPANT DETAILS

Bacterial cultures

Bacterial cultures were handled as described[8]. Briefly, plasmids for protein expression were transformed into *E. coli* BL21 CodonPlus (DE3) RIPL cells (Agilent). Cultures grown in Terrific Broth were induced with 0.1 mM isopropyl β-D-thiogalactopyranoside (IPTG) at an OD600 of 0.8 and then transferred to 16°C for 16 h.

METHOD DETAILS

Plasmids

Plasmids were prepared as described[8]. Briefly, wild-type Cdc48/p97 and their variants were cloned into the pET28 vector with an N-terminal His6-tag and a TEV-protease cleavage site. For Cdc48 pull-down experiments, two copies of strep tag (WSHPQFEK) were added at its C-terminus. Ufd1 was cloned into the pK27 vector followed by an N-terminal His14-SUMO (small ubiquitin-like modifier) tag, as described[8]. Npl4 was cloned into the pET21 vector with a C-terminal His6-tag or FLAG-His6 (DYKDDDDKGLEHHHHHH) tag, as described[8].

Wild-type Otu1/Yod1 and their variants were cloned into the pET28 vector with an N-terminal His6-tag and a TEV-protease cleavage site followed by a FLAG tag. Wild-type Ubx5 or UBXN7 was cloned into the pET28 vector with an N-terminal His6-tag and a C-terminal SBP tag.

A bacterial expression plasmid coding for an N-end degron (NeD) sequence with lysine-less super-folder GFP (NeD-sfGFP) and Ub(n)-FOLD has been described[5,8].

Protein purifications

364 Protein purification was performed as described[8]. Briefly, bacterial cells were harvested by
365 centrifugation at 5,000 x g for 10 min at 4°C and resuspended in cold wash buffer (50 mM
366 Tris-HCl, pH 8, 320 mM NaCl, 5 mM $MgCl_2$, 10 mM imidazole, 0.5 mM ATP) supplemented
367 with phenylmethylsulfonyl fluoride (PMSF; 1 mM) and a protease inhibitor cocktail, and
368 lysed by sonication. After ultracentrifugation, the supernatant was incubated with Ni-NTA
369 resin that was pre-equilibrated with wash buffer. The beads were washed three times with
370 wash buffer and protein eluted with elution buffer (50 mM Tris-HCl, pH 8, 150 mM NaCl, 5
371 mM $MgCl_2$, 400 mM imidazole). The eluted protein was concentrated and subjected to size-
372 exclusion chromatography (SEC).

373 Untagged Ufd1/Npl4 (UN) complex, Ub-G76V-Dendra, and NeD-sfGFP were purified as
374 described[8]. FLAG-26S proteasomes were expressed in yeast cells and purified as
375 described[8,27]. *S. cerevisiae* ubiquitin was purchased from Boston Biochem.
376 Photoconversion, dye labeling, and *in vitro* ubiquitination of Ub-G76V-Dendra (for Ub(n)-
377 FOLD), and dye labeling and *in vitro* ubiquitination of NeD-sfGFP (for Ub(n)-TAIL) have been
378 described[8,10].

379 **Substrate degradation assays**

380 Substrate degradation assays were carried out as described[8]. Briefly, 100 nM of
381 fluorescently labeled substrate was mixed with 200 nM 26S proteasomes, Cdc48, UN,
382 Otu1, Rad23, or Ubx5 in 26S reaction buffer (60 mM HEPES, pH 7.4, 20 mM NaCl, 20 mM
383 KCl, 10 mM $MgCl_2$, 2.5% glycerol, and 1 mM TCEP) and 0.5 mg/ml protease-free bovine
384 serum albumin (BSA). The reaction was incubated with an ATP regeneration mixture (5 mM
385 ATP, 16 mM creatine phosphate, 0.03 mg/mL creatine kinase) for 1 h. The samples were
386 subjected to SDS-PAGE, followed by fluorescence scanning on an Odyssey imager (LI-
387 COR).

388 **Pull-down experiments**

389 The two-step pull-down experiments in Figure 1F were performed, as described[8], with
390 some modifications. Briefly, 5 µl pre-equilibrated FLAG antibody M2 agarose beads (Sigma)
391 were first incubated with 0.2 µM Cdc48, 0.2 µM Ufd1, 0.2 µM Npl4-FLAG, 0.2 µM
392 polyubiquitinated substrate in 26S reaction buffer supplemented with 5 mM ADP for 1 h at
393 4°C. The beads were washed three times with 26S reaction buffer. The beads were then
394 incubated with 0.2 µM Otu1, 26S proteasomes, or Rad23 in 26S reaction buffer
395 supplemented with ATP for 20 min at 30°C. The beads were washed again and proteins
396 were eluted with 20 µl of 26S reaction buffer supplemented with 0.2 mg/ml 3xFLAG peptide
397 (Bimake). The eluted samples were subjected to SDS-PAGE, followed by fluorescence
398 scanning and Coomassie-blue staining.

399 The pull-down experiments in Figure 2A were performed as described[8], with the following
400 modifications. 10 µl pre-equilibrated FLAG antibody M2 agarose beads (Sigma) were
401 incubated with 1 µM Otu1-C120S-FLAG, 1 µM Cdc48, 1 µM UN, 1 µM Ubx5, and 1 µM Ub(n)-
402 TAIL in SEC buffer supplemented with 5 mM ATPγS for 1 h at 4°C. The beads were washed

403 three times with SEC buffer and bead-bound proteins were eluted with 20 µl of SEC buffer
404 supplemented with 0.2 mg/ml 3xFLAG peptide (Bimake).

405 For the pull-down experiments in Figure 2B, a mixture of 1 uM Cdc48 and 1 uM UN in 5 mM
406 ADP was mixed and incubated for 0.5 h at 4°C. 10 µl pre-equilibrated FLAG antibody M2
407 agarose beads (Sigma) were incubated with 1 µM Otu1-C120S or Otu1-ΔUBXL-C120S in
408 SEC buffer for 1 h at 4°C. The beads were washed three times with SEC buffer followed by
409 incubation with the pre-assembled Cdc48-UN complex for 1 h at 4°C. The beads were
410 washed three times with SEC buffer and bead-bound proteins were eluted with 20 µl of
411 SEC buffer supplemented with 0.2 mg/ml 3xFLAG peptide (Bimake). The eluted samples
412 were subjected to SDS-PAGE, followed by Coomassie-blue staining.

413 For the pull-down experiments in Figure 2C, 10 µl pre-equilibrated streptavidin agarose
414 beads (Thermo Fisher) were incubated with 1 µM UBXN7-SBP, 1 µM p97, 1 µM human UN, 1
415 µM Yod1-C160S, and 1 µM Ub(n)-TAIL in SEC buffer supplemented with 5 mM ATPγS for 1 h
416 at 4°C. The beads were washed three times with SEC buffer and bead-bound proteins were
417 eluted with 20 µl of SEC buffer supplemented with 2 mM biotin.

418

419 **Cryo-EM sample preparation and data collection**

420 100 µl pre-equilibrated streptavidin agarose beads (Thermo Fisher) were incubated with 1
421 mL mixture of 0.2 µM UBXN7-SBP, 0.2 µM p97-E578Q, 0.2 µM human UN, 0.2 µM Yod1-
422 C160S, and 0.2 µM Ub(n)-TAIL in SEC buffer supplemented with 5 mM ATP for 1.5 h at 4°C.
423 The beads were washed three times with SEC buffer supplemented with ATP, and bead-
424 bound proteins were eluted with 300 µl of SEC buffer supplemented with 2 mM biotin and 5
425 mM ATP. The eluted proteins were concentrated to 30 µl and incubated with 0.05%
426 glutaraldehyde for 30 min at room temperature. The reaction was quenched with 40 mM
427 Tris pH 7.5.

428 All samples for cryo-EM were prepared with a Thermo Fisher Vitrobot Mark IV system,
429 maintained at 100% humidity at 4°C. Blot times of 5.0 s were used 30s after 3 µl sample
430 application to Quantifoil Au 1.2/1.3 200 mesh grids that had previously been plasma-
431 treated in a Pelco easiGlow at 0.39 mBar, 15 mA for 60 s.

432 6,426 micrographs were collected on a Thermo Fisher Titan Krios operating at 300 kV, with
433 GIF BioQuantum energy filter and a Gatan K3 camera in super resolution mode (super
434 resolution pixel size of 0.4135 Å/pixel). The total exposure time of 10 s was divided into 50
435 frames (total dose of approximately 50 ($e^-/Å^2$), with a defocus range of −0.8 µm to −2.0 µm.
436 The objective and C2 apertures were set to 70 µm.

437 **Image processing**

438 All subsequent image processing steps were carried out using Cryosparc[28]. Frame
439 alignment and dose-weighting was carried out using Patch Motion Correction. CTF
440 correction was performed with Patch CTF. Density visualization was performed using UCSF
441 ChimeraX[29].

After picking a total of 2,044,375 particles, an initial round of 2D classification resulted in 801,542 particles, which were subjected to heterogeneous refinement. One class of 361,890 particles was selected for further analysis. The particles were sub-classified, resulting in two classes totaling 113,094 particles. This class was then sub-classified into two classes, one of which was chosen for further processing based on the density for Npl4. The resulting 65,959 particles were subjected to refinement and gave rise to a map of 2.97 Å resolution. To better visualize the Npl4 tower, the initial model was locally refined with a mask containing the p97 D1 ring and the Npl4 tower, resulting in a 3.05 Å map, where the D2 ring density was significantly weaker in local resolution compared to the rest of the density.

Model Building

Initial models were built into the map using existing structures of p97 (PDB: 7LMZ)[6], human Ufd1 (PDB: 7WWQ)[13], human Npl4 (AlphaFold Database: AF-Q8TAT6-F1)[30], and unfolded ubiquitin (PDB: 6OA9)[4] with rigid body fitting. Model building was then carried out in Coot. Amino acid side chain positions were modified based on the density.

For the model shown in Figure 4 and figure S3, the structure of ubiquitin molecules (PDB: 6OA9)[4] was fit as a rigid-body into the density. The structures of p97 N domains (PDB: 7R7S)[16] were fit as rigid-bodies into the density of subunits A, C, and F. The structure of human Ufd1 SHP1 motif was modeled after a SHP1-N domain structure (PDB: 5B6C)[31].

QUANTIFICATION AND STATISTICAL ANALYSIS

Quantification of bands after fluorescence scanning of gels was carried out using the ImageStudio software (LI-COR) as described[8].

REFERENCES

1 Collins, G. A. & Goldberg, A. L. The Logic of the 26S Proteasome. *Cell* **169** (2017/05/18). https://doi.org:10.1016/j.cell.2017.04.023

2 Davis, C., Spaller, B. L. & Matouschek, A. Mechanisms of substrate recognition by the 26S proteasome. *Curr Opin Struct Biol* **67**, 161-169 (2021). https://doi.org:10.1016/j.sbi.2020.10.010

3 Bodnar, N., Rapoport, T., Bodnar, N. & Rapoport, T. Toward an understanding of the Cdc48/p97 ATPase. *F1000Research 2017 6:1318* **6** (2017/08/03). https://doi.org:10.12688/f1000research.11683.1

4 EC, T. *et al.* Substrate processing by the Cdc48 ATPase complex is initiated by ubiquitin unfolding - PubMed. *Science (New York, N.Y.)* **365** (08/02/2019). https://doi.org:10.1126/science.aax1033

5 Ji, Z. *et al.* Translocation of polyubiquitinated protein substrates by the hexameric Cdc48 ATPase. *Mol Cell* **82**, 570-584 e578 (2022). https://doi.org:10.1016/j.molcel.2021.11.033

6 Pan, M. *et al.* Mechanistic insight into substrate processing and allosteric inhibition of human p97. *Nat Struct Mol Biol* **28**, 614-625 (2021). https://doi.org:10.1038/s41594-021-00617-2

7 Pan, M. *et al.* Seesaw conformations of Npl4 in the human p97 complex and the inhibitory mechanism of a disulfiram derivative. *Nature Communications 2021 12:1* **12** (2021-01-05). https://doi.org:10.1038/s41467-020-20359-x

8 H, L., Z, J., JA, P., SP, G. & TA, R. Bidirectional substrate shuttling between the 26S proteasome and the Cdc48 ATPase promotes protein degradation - PubMed. *Molecular cell* **84** (04/04/2024). https://doi.org:10.1016/j.molcel.2024.01.029

9 Bodnar, N. O. & Rapoport, T. A. Molecular mechanism of substrate processing by the Cdc48 ATPase complex. *Cell* **169** (2017/05/05). https://doi.org:10.1016/j.cell.2017.04.020

10 Ji, Z. *et al.* Translocation of polyubiquitinated protein substrates by the hexameric Cdc48 ATPase. *Molecular Cell* **82** (2022/02/03). https://doi.org:10.1016/j.molcel.2021.11.033

11 Stein, A., Ruggiano, A., Carvalho, P. & Rapoport, T. A. Key steps in ERAD of luminal ER proteins reconstituted with purified components. *Cell* **158**, 1375-1388 (2014). https://doi.org:10.1016/j.cell.2014.07.050

12 Bruderer, R. M., Brasseur, C. & Meyer, H. H. The AAA ATPase p97/VCP interacts with its alternative co-factors, Ufd1-Npl4 and p47, through a common bipartite binding mechanism. *J Biol Chem* **279**, 49609-49616 (2004). https://doi.org:10.1074/jbc.M408695200

13 Nguyen, T. Q. *et al.* Structural basis for the interaction between human Npl4 and Npl4-binding motif of human Ufd1. *Structure* **30**, 1530-1537 e1533 (2022). https://doi.org:10.1016/j.str.2022.08.005

14 Abramson, J. *et al.* Accurate structure prediction of biomolecular interactions with AlphaFold 3. *Nature* **630**, 493-500 (2024). https://doi.org:10.1038/s41586-024-07487-w

15 Dreveny, I., Kondo, H., Uchiyama, K., Shaw, A., Zhang, X. & Freemont, P. S. Structural basis of the interaction between the AAA ATPase p97/VCP and its adaptor protein p47. *EMBO J* **23**, 1030-1039 (2004). https://doi.org:10.1038/sj.emboj.7600139

16 Nandi, P. *et al.* Structural and Functional Analysis of Disease-Linked p97 ATPase Mutant Complexes. *Int J Mol Sci* **22** (2021). https://doi.org:10.3390/ijms22158079

17 Kochańczyk, T. *et al.* Structural basis for transthiolation intermediates in the ubiquitin pathway. *Nature 2024 633:8028* **633** (2024-08-14). https://doi.org:10.1038/s41586-024-07828-9

18 Kochenova, O. V., Mukkavalli, S., Raman, M. & Walter, J. C. Cooperative assembly of p97 complexes involved in replication termination. *Nat Commun* **13**, 6591 (2022). https://doi.org:10.1038/s41467-022-34210-y

19 Verma, R. *et al.* Role of Rpn11 metalloprotease in deubiquitination and degradation by the 26S proteasome. *Science* **298**, 611-615 (2002). https://doi.org:10.1126/science.1075898

20 Yao, T. & Cohen, R. E. A cryptic protease couples deubiquitination and degradation by the proteasome. *Nature* **419**, 403-407 (2002). https://doi.org:10.1038/nature01071

21 Hanzelmann, P., Buchberger, A. & Schindelin, H. Hierarchical binding of cofactors to the AAA ATPase p97. *Structure* **19**, 833-843 (2011). https://doi.org:10.1016/j.str.2011.03.018

22 Lee, H. G., Lemmon, A. A. & Lima, C. D. SUMO enhances unfolding of SUMO-polyubiquitin-modified substrates by the Ufd1/Npl4/Cdc48 complex. *Proc Natl Acad Sci U S A* **120**, e2213703120 (2023). https://doi.org:10.1073/pnas.2213703120

23 Kilgas, S. & Ramadan, K. Inhibitors of the ATPase p97/VCP: From basic research to clinical applications. *Cell Chemical Biology* **30** (2023/01/19). https://doi.org:10.1016/j.chembiol.2022.12.007

24 H, L. *et al.* A p97/Valosin-Containing Protein Inhibitor Drug CB-5083 Has a Potent but Reversible Off-Target Effect on Phosphodiesterase-6 - PubMed. *The Journal of pharmacology and experimental therapeutics* **378** (2021 Jul). https://doi.org:10.1124/jpet.120.000486

25 Nie, P. *et al.* Targeting p97-Npl4 interaction inhibits tumor T(reg) cell development to enhance tumor immunity. *Nat Immunol* **25**, 1623-1636 (2024). https://doi.org:10.1038/s41590-024-01912-y

26 Okatsu, K. *et al.* Adaptor-Specific Peptide Inhibitors of the Ubiquitin-Chain-Dependent Unfolding Activity of the Human p97(VCP)-UFD1-NPL4 Complex. *J Med Chem* **68**, 11270-11278 (2025). https://doi.org:10.1021/acs.jmedchem.5c00201

27 de la Pena, A. H., Goodall, E. A., Gates, S. N., Lander, G. C. & Martin, A. Substrate-engaged 26S proteasome structures reveal mechanisms for ATP-hydrolysis-driven translocation. *Science* **362** (2018). https://doi.org:10.1126/science.aav0725

28 Punjani, A., Rubinstein, J. L., Fleet, D. J. & Brubaker, M. A. cryoSPARC: algorithms for rapid unsupervised cryo-EM structure determination. *Nat Methods* **14**, 290-296 (2017). https://doi.org:10.1038/nmeth.4169

29 Meng, E. C. *et al.* UCSF ChimeraX: Tools for structure building and analysis. *Protein Sci* **32**, e4792 (2023). https://doi.org:10.1002/pro.4792

30 Jumper, J. *et al.* Highly accurate protein structure prediction with AlphaFold. *Nature 2021 596:7873* **596** (2021-07-15). https://doi.org:10.1038/s41586-021-03819-2

31 Le, L. T., Kang, W., Kim, J. Y., Le, O. T., Lee, S. Y. & Yang, J. K. Structural Details of Ufd1 Binding to p97 and Their Functional Implications in ER-Associated Degradation. *PLoS One* **11**, e0163394 (2016). https://doi.org:10.1371/journal.pone.0163394

ACKNOWLEDGEMENTS

We thank R. Yan at the HHMI Janelia Research Campus cryo-EM facility for assistance with microscope operation and data collection, Z. Li, R. Walsh, C. Leistner, M. Mayer, R. Nair, and S. Rawson at the Harvard cryo-EM Center for Structural Biology for

assistance with sample preparation, microscope operation, data collection, and image processing, the SBGrid team for software and workstation support. This work was supported by a NIGMS grant (R01 GM052586) to T.A.R. T.A.R. is a Howard Hughes Medical Institute Investigator.

FUNDING DECLARATION

This work was supported by a NIGMS grant (R01 GM052586) to T.A.R. T.A.R. is a Howard Hughes Medical Institute Investigator.

This manuscript is the result of funding in whole or in part by the National Institutes of Health (NIH). It is subject to the NIH Public Access Policy. Through acceptance of this federal funding, NIH has been given a right to make this manuscript publicly available in PubMed Central upon the Official Date of Publication, as defined by NIH.

AUTHOR CONTRIBUTIONS

H.L. performed all experiments, H.G. helped with cryo-EM sample preparation and data processing, T.A.R. supervised the project. H.L. and T.A.R. wrote the manuscript.

DATA AVAILABILITY STATEMENT

Cryo-EM maps have been deposited in the Electron Microscopy Data Bank (EMDB, www.ebi.ac.uk/pdbe/emdb/) under the accession codes EMD-73365 (composite map), EMD- 73375 (globally refined map), and EMD-73376 (map locally refined on p97 D1 and Npl4). The atomic model has been deposited in the Protein Data Bank under the accession codes PDB 9YRC.

DECLARATION OF INTERESTS

The authors declare no competing interests.

590 **Figure legends**

591 **Fig. 1. Otu1 stimulates substrate transfer from the Cdc48 ATPase to the 26S**
592 **proteasome.**

593 (**A**) Fluorescently labeled Ub(n)-TAIL was incubated for 60 min with 26S proteasomes.
594 Where indicated, Cdc48-UN and different concentrations of Otu1 (given relative to that
595 of proteasomes) were added. The samples were analyzed by SDS-PAGE, followed by
596 fluorescence scanning. The percentage of substrate degraded was quantified by
597 determining the fluorescence in peptides (after background subtraction) and comparing
598 it to the total fluorescence in each lane of the SDS gel.

599 (**B**) As in (A), but with Ub(n)-FOLD and incubation with both proteasomes and Cdc48-
600 UN. Where indicated, Otu1, an enzymatically inactive Otu1 mutant (Otu1-C120S), or
601 Ubx5 were added.

602 (**C**) As in (B), but with Ub(n)-TAIL.

603 (**D**) As in (B), but with the addition of either full-length Otu1 or Otu1-ΔUBXL.

604 (**E**) As in (A), but with Ub(n)-TAIL and either wild-type (WT) Cdc48 or the indicated
605 mutants. Otu1 was added at the same concentration as proteasomes.

606 (**F**) Fluorescently labeled Ub(n)-TAIL was incubated in the presence of ATP with beads
607 containing streptavidin (Strep)-tagged Cdc48-UN complex (1st incub.). The beads were
608 washed and were then incubated with 26S proteasomes and Rad23 or Otu1, as
609 indicated (2nd incub.). The bound material remaining on the beads was analyzed by
610 SDS-PAGE, followed by fluorescence scanning (upper panel) and Coomassie-blue
611 staining (lower panel). Bound substrate was quantified relative to the material bound in
612 the presence of buffer (lane 1 set to 100%).

613 **Fig. 2. Otu1 binds to the Cdc48 ATPase simultaneously with other cofactors.**

614 (**A**) Cdc48-UN was incubated in the presence of ATPγS with different combinations of
615 Ub(n)-TAIL, Otu1-C120S-FLAG, and Ubx5, as indicated. The samples were incubated
616 with beads containing anti-FLAG antibodies and the bound material analyzed by SDS-
617 PAGE, followed by fluorescence scanning (upper panel) and Coomassie-blue staining
618 (lower panel).

619 (**B**) Cdc48-UN was incubated with wild-type Otu1-C120S-FLAG or a mutant lacking the
620 UBXL domain. The samples were incubated with beads containing anti-FLAG
621 antibodies and the bound material analyzed by SDS-PAGE, followed by Coomassie-
622 blue staining.

623 (**C**) Human p97 ATPase, human UN complex, and UBXN7 (Ubx5 homolog) were mixed
624 and incubated with Yod1-C160S (Otu1 homolog) and Ub(n)-TAIL substrate, as

625 indicated. The samples were incubated with streptavidin beads, and the bound material
626 analyzed by SDS-PAGE followed by Coomassie-blue staining. Lanes 1-5 shows the
627 purity of the components.

628 **Fig. 3. Cryo-EM structure of substrate-engaged p97 ATPase with cofactors.**

629 (**A**) A complex containing human p97 ATPase, hNpl4/hUfd1, UBXN7, Yod1, and poly-
630 ubiquitinated substrate (Ub(n)-TAIL) was purified and subjected to cryo-EM single-
631 particle analysis. The left two panels show the density map of the best particle class in
632 two different side views. p97 is shown in grey, hUfd1 in blue, Npl4 in orange, and the
633 unfolded ubiquitin molecule (unUb) in yellow. The right two panels show the
634 corresponding models as cartoons. Ufd1 and unUb are shown as space-filling models.

635 (**B**) The regions indicated as 1 and 2 in the left panel are magnified in the two right
636 panels to show the density of unUb in the Npl4 groove (1) and the central pore of p97
637 (2). Some residues of unUb are labeled.

638 (**C**) Arrangements of the six protomers (A to F) in the D1 and D2 rings. The positions of
639 the nucleotide in each protomer are labeled. Note that D1 ring is almost planar, while
640 the protomers of the D2 ring are arranged as a staircase.

641 (**D**) Boxed areas 1 and 2 in the left panel are magnified and the corresponding models
642 are shown on the left. ubUb is shown as a stick model. The pore loops of the D1 ring
643 (inset #1) are shown in different colors. The aromatic pore loop residues in the D2 ring
644 (inset #2) are shown as stick models.

645

646 **Fig. 4. Interactions of the N domain of p97.**

647 (**A**) The cryo-EM map was locally refined based on a mask containing the Npl4 tower,
648 the D1 ring, and three N domains. The composite map of the locally refined map and
649 the overall map are shown in three different views. p97 is shown in grey, Ufd1 in blue,
650 Npl4 in orange, the unfolded ubiquitin molecule (unUb) in yellow, and the following two
651 folded ubiquitin molecules (Ub1 and Ub2) in cyan. In the right most panel, the visible
652 three N domains are shown in green.

653 (**B**) Models for Ub1 and Ub2 are shown as cyan ribbons. The corresponding ubiquitin
654 molecules of the yeast complex are shown as pink ribbons, based on an alignment of
655 Cdc48-UN (PDB: 6OA9)[4] with p97-UN. RMSD values were calculated for each pair of
656 ubiquitin molecules.

657 (**C**) Magnified view of the arrangement of Ub1 and Ub2. Note that in the human complex
658 (cyan) K48 of Ub1 is close to G76 of Ub2, whereas in the yeast complex (pink) the

659 distance is too large for the two ubiquitin molecules to be linked (dashed lines with
660 labeled distance).

661

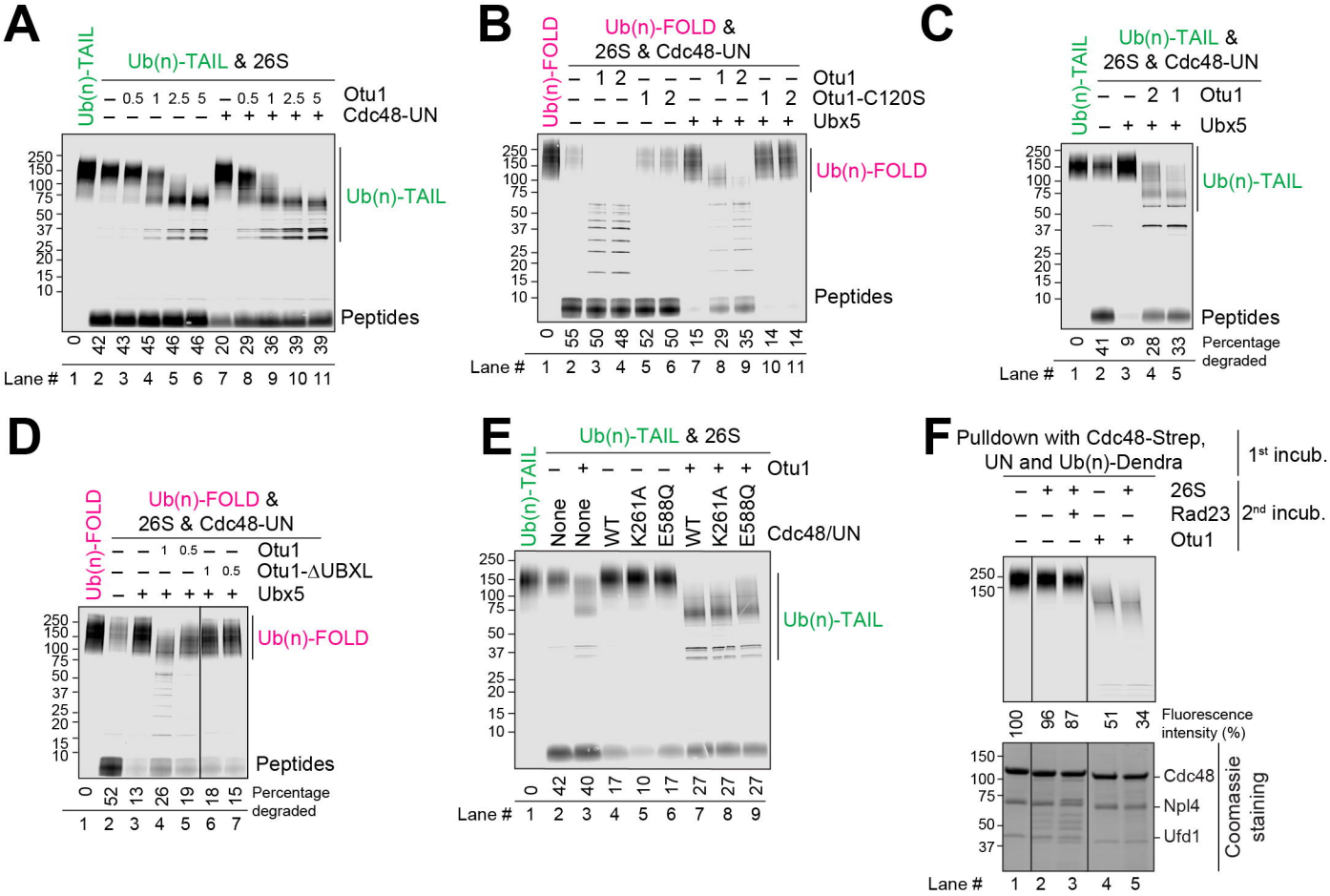
A
Ub(n)-TAIL & 26S
Ub(n)-TAIL
Otu1
Cdc48-UN
Ub(n)-TAIL
Peptides
Lane #
B
Ub(n)-FOLD & 26S & Cdc48-UN
Ub(n)-FOLD
Otu1
Otu1-C120S
Ubx5
Ub(n)-FOLD
Peptides
Lane #
C
Ub(n)-TAIL & 26S & Cdc48-UN
Ub(n)-TAIL
Otu1
Ubx5
Ub(n)-TAIL
Peptides
Percentage degraded
Lane #
D
Ub(n)-FOLD & 26S & Cdc48-UN
Ub(n)-FOLD
Otu1
Otu1-ΔUBXL
Ubx5
Ub(n)-FOLD
Peptides
Percentage degraded
E
Ub(n)-TAIL & 26S
Ub(n)-TAIL
Otu1
None
None
WT
K261A
E588Q
WT
K261A
E588Q
Cdc48/UN
Ub(n)-TAIL
Lane #
F
Pulldown with Cdc48-Strep, UN and Ub(n)-Dendra
1st incub.
26S
Rad23
Otu1
2nd incub.
Fluorescence intensity (%)
Cdc48
Npl4
Ufd1
Coomassie staining
Lane #

Figure 1

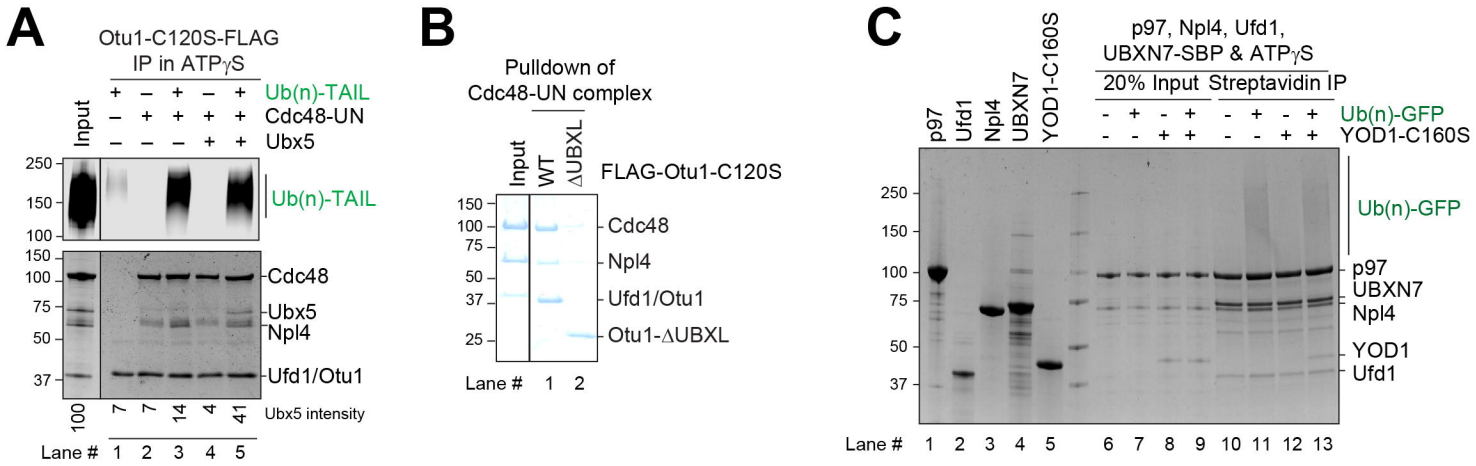
A
Otu1-C120S-FLAG
IP in ATPγS
Input
Ub(n)-TAIL
Cdc48-UN
Ubx5
250
150
100
Ub(n)-TAIL
150
100
75
50
37
Cdc48
Ubx5
Npl4
Ufd1/Otu1
100
7
7
14
4
41
Ubx5 intensity
Lane # 1 2 3 4 5
B
Pulldown of
Cdc48-UN complex
Input
WT
ΔUBXL
FLAG-Otu1-C120S
150
100
75
50
37
25
Cdc48
Npl4
Ufd1/Otu1
Otu1-ΔUBXL
Lane # 1 2
C
p97
Ufd1
Npl4
UBXN7
YOD1-C160S
p97, Npl4, Ufd1,
UBXN7-SBP & ATPγS
20% Input
Streptavidin IP
Ub(n)-GFP
YOD1-C160S
250
150
100
75
50
37
Ub(n)-GFP
p97
UBXN7
Npl4
YOD1
Ufd1
Lane # 1 2 3 4 5 6 7 8 9 10 11 12 13

Figure 2

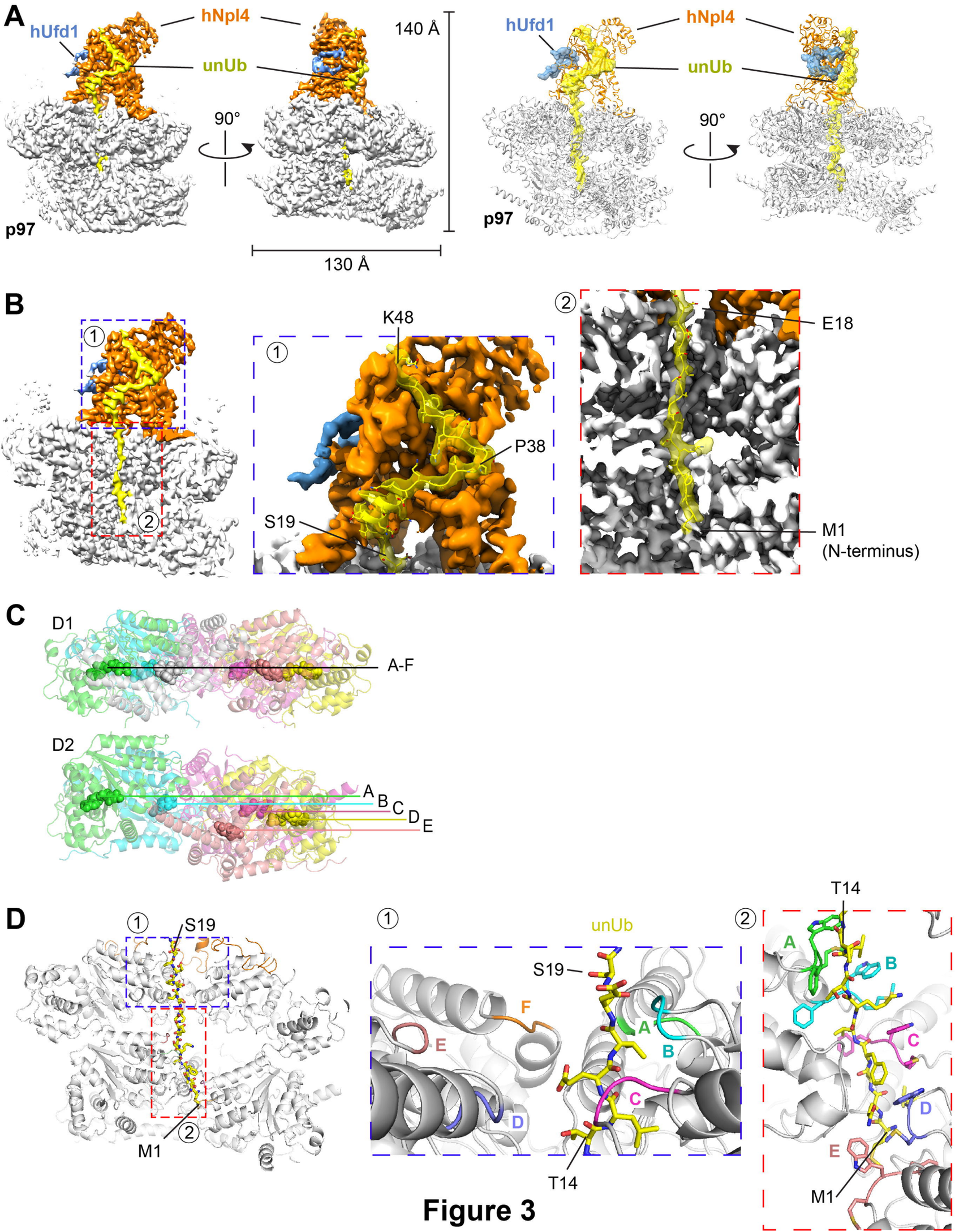
A
hUfd1
hNpl4
unUb
140 Å
90°
p97
130 Å
B
1
2
K48
P38
S19
E18
M1
(N-terminus)
C
D1
A-F
D2
A
B
C
D
E
D
S19
M1
unUb
F
T14

Figure 3

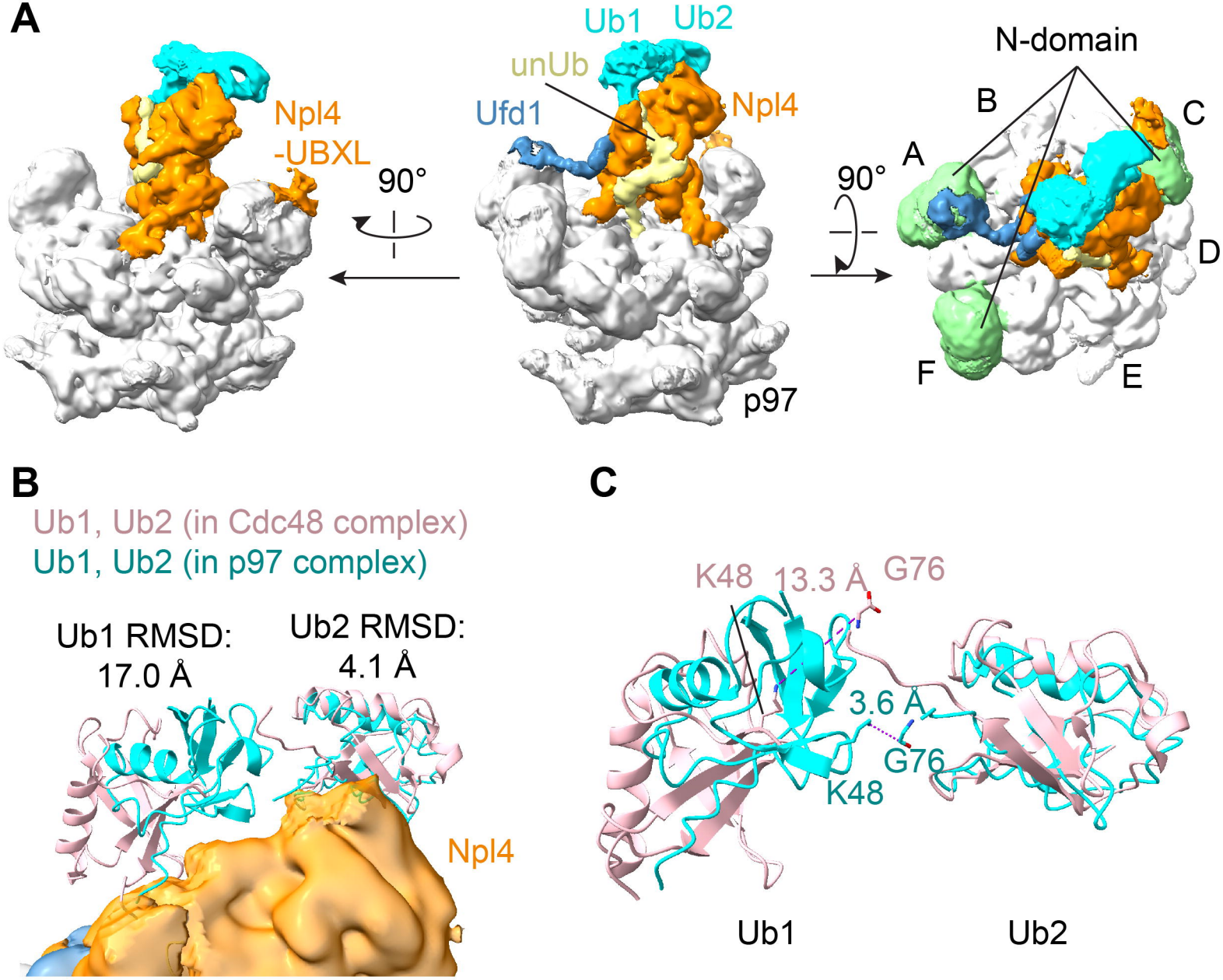
A
Npl4
-UBXL
90°
Ub1
Ub2
unUb
Ufd1
Npl4
p97
90°
N-domain
A
B
C
D
E
F
B
Ub1, Ub2 (in Cdc48 complex)
Ub1, Ub2 (in p97 complex)
Ub1 RMSD:
17.0 Å
Ub2 RMSD:
4.1 Å
Npl4
C
K48
13.3 Å
G76
3.6 Å
G76
K48
Ub1
Ub2

Figure 4